Chemical Engineering Journal 374 (2019) 958–964

Contents lists available at ScienceDirect

Chemical Engineering Journal

journal homepage: www.elsevier.com/locate/cej

Substrate oxidation enhances the electrochemical production of hydrogen peroxide

Jonghun Lim, Michael R. Hoffmann*

Linde + Robinson Laboratories, California Institute of Technology, Pasadena, CA 91125, United States

HIGHLIGHTS

- The electrochemical production of H_2O_2 is enhanced in the presence of organic electron donors (*i.e.*, pollutants).
- The oxidation of organic substrates prevents the anodic decomposition of H_2O_2.
- The production of H_2O_2 with simultaneous organic pollutants degradation is more efficient under acidic conditions.

GRAPHICAL ABSTRACT

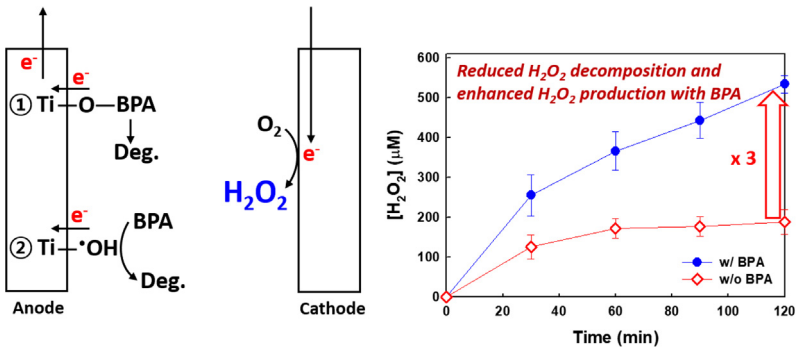

ARTICLE INFO

Keywords:
Electrocatalysis
Hydrogen peroxide
Anodic decomposition of H_2O_2
Organic electron donors

ABSTRACT

Hydrogen peroxide (H_2O_2) is electrochemically produced via oxygen (O_2) reduction on a carbon cathode surface. In order to enhance the production of H_2O_2, anodic loss pathways, which significantly reduce the overall H_2O_2 production rate, should be inhibited. In this study, we investigate the effects of organic electron donors (*i.e.*, typical chemical contaminants) on the anodic loss pathways of H_2O_2 in a single-cell electrochemical reactor that employs an anode composed of TiO_2 over-coated on a mixed-metal oxide ohmic contact catalyst, $Ir_{0.7}Ta_{0.3}O_2$, deposited on a Ti-metal that is coupled with a graphite rod cathode in a sodium sulfate (Na_2SO_4) electrolyte that is saturated with oxygen (O_2). Organic electron donors are shown to enhance the electrochemical production of H_2O_2, while simultaneously undergoing oxidative degradation. The observed positive effect of organic electron donors on the electrochemical production of H_2O_2 is due in part to a preferential adsorption of organic substrates on the TiO_2 outer layer of the anode. The sorption of the organic electron donors inhibits the formation of surficial titanium hydroperoxo species (≡Ti-OOH) on the anode surface. The organic sorbates also act as scavengers of surface-bound hydroxyl radical ≡Ti-OH. As a result, the decomposition of H_2O_2 on the anode surface is significantly reduced. The cathodic production rate of H_2O_2 at low pH is enhanced due to proton coupled electron transfer (PCET) to O_2, while the anodic decomposition of H_2O_2 is inhibited due to electrostatic interactions between negatively-charged organic substrates and a positively-charged outer surface of the anode (TiO_2 pH_{zpc} = 5.8) at low pH.

* Corresponding author.
E-mail address: mrh@caltech.edu (M.R. Hoffmann).

https://doi.org/10.1016/j.cej.2019.05.165
Received 6 February 2019; Received in revised form 22 May 2019; Accepted 24 May 2019
Available online 25 May 2019

1. Introduction

Hydrogen peroxide (H_2O_2) is often used as an eco-friendly oxidant because it is reduced to water as an electron acceptor and readily decomposes to water and oxygen (O_2) [1]. The high oxidation potential ($E_0 = +1.76\ V_{NHE}$) of H_2O_2 allows for the direct oxidation of certain organic and inorganic electron donors and for the indirect oxidation by hydroxyl radical produced via the UV photolysis of H_2O_2 or by Fenton-reagent activation [2]. Hydrogen peroxide is also used in organic syntheses, liquid fuel rocket propulsion, disinfection, and environmental remediation [1]. Moreover, H_2O_2 is frequently used in advanced oxidation processes for water or air [3–5].

Hydrogen peroxide is normally produced by the anthraquinone method involving a multistep oxidation of 2-ethyl-9,10-dihydroxyanthracene and the subsequent hydrogenation of 2-ethylanthraquinone [6]. However, this method is not environmentally benign because hydrogen (H_2) gas, organic solvents, and high energy inputs are required. The direct reaction between the H_2 and O_2 gas using metal-based catalysts (*e.g.*, Au or Pd/Au alloys) in acid or methanolic solutions has been investigated as an alternative method for H_2O_2 production but this method is also not environmentally and economically viable [7,8] due to the explosion potential of the H_2 and O_2 gaseous mixture [9,10]. In contrast, the electrochemical production of H_2O_2 via a two-electron transfer to O_2 is relatively benign synthetic method since it takes place at low temperatures and pressures [11].

Two pathways are available for the electrochemical generation of H_2O_2: (1) reduction of O_2 on an appropriate cathode (Eq. (1)) [11] and (2) oxidation of water on a suitable anode material (*e.g.*, an anode with a high overpotential for the OER) (Eq. (2)) [12].

$$O_2 + 2H^+ + 2e^- \rightarrow H_2O_2 \quad (1)$$

$$2H_2O \rightarrow H_2O_2 + 2H^+ + 2e^- \quad (2)$$

Anodes and cathodes optimized for H_2O_2 production have been developed [13–16]. However, the electrochemical synthesis of H_2O_2 is still limited by the decomposition of H_2O_2 on the surfaces of both the cathode (Eqs. (3) and (4)) and anode (Eqs. (5)–(7)) [17].

$$H_2O_2 + e^- + H^+ \rightarrow H_2O + {}^{\cdot}OH \quad (3)$$

$$H_2O_2 + 2H^+ + 2e^- \rightarrow 2H_2O \quad (4)$$

$$H_2O_2 \rightarrow HO_2^{\cdot} + H^+ + e^- \quad (5)$$

$$H_2O_2 \rightarrow O_2 + 2H^+ + 2e^- \quad (6)$$

$$H_2O_2 + HO^{\cdot} \rightarrow HOO^{\cdot} + H_2O \quad (7)$$

In order to improve the overall yield of H_2O_2 during the electrochemical production, the decomposition of H_2O_2 should be substantially reduced. For example, carbon-based cathodes have been used since they inhibit the cathodic decomposition of H_2O_2 [18]. However, the strategy for preventing the anodic decomposition of H_2O_2 has received little attention.

In this study, we investigate the effect of organic electron donors on the electrochemical production of H_2O_2 as a method to inhibit the anodic decomposition of H_2O_2. Our hypothesis is that the production of H_2O_2 should be enhanced in the presence of organic electron donors at a constant cathodic potential. Organic substrates should prevent the anodic decomposition of H_2O_2 with respect to further anodic oxidation to superoxide and oxygen. The impact of experimental variables including applied voltage, pH, and probe reagents on the production of H_2O_2 in the presence of specific organic electron donors is explored.

2. Materials and methods

2.1. Materials and chemicals

A dimensionally-stable anode consisting of $Ir_{0.7}Ta_{0.3}O_2$ formed during *in situ* spray pyrolysis of precursor reagents on a heated titanium metal substrate and over-coated with TiO_2 was used ($TiO_2/Ir_{0.7}Ta_{0.3}O_2$/Ti). This composite anode formulation has been shown to be active with respect to both the chlorine and oxygen evolution reactions [19]. The aqueous-phase precursor solutions were composed of 3.5 mM $IrCl_3$ and 1.5 mM $TaCl_5$ in isopropanol for formation of the $Ir_{0.7}Ta_{0.3}O_2$ layer, while the TiO_2 overcoating layer was formed using a 25 mM titanium-glycolate solution for deposition of the overcoating TiO_2 layer was deposited by spray coating of the solution directly on to Ti foil heated to 300 °C. The resulting film was annealed at 500 °C for 10 min. These procedures were repeated to reach a targeted mass loading. Upon achieving the desired mass loading, the final composite was annealed at 500 °C for 1 h. Chemical reagents used in this study were as follows: sodium sulfate (Na_2SO_4, Sigma-Aldrich), bisphenol A (BPA, Aldrich), phenol (J. T. Baker), 4-chlorophenol (4-CP, Sigma-Aldrich), coumarin (Sigma), potassium bis(oxalato)-oxotitanate (IV) dihydrate ($K_2[TiO(C_2O_4)_2]\cdot 2H_2O$, Alfa Aesar), sulfuric acid (H_2SO_4, J. T. Baker), hydrogen peroxide (H_2O_2 (30 wt%), Sigma-Aldrich). All chemical reagents were used as received without any purification. Deionized water was used as solution and prepared by a Millipore system (≥18 MΩ·cm, Milli-Q).

3. Electrochemical experiments

A three-electrode configuration including a working electrode (graphite rod, diameter 6 mm), a counter electrode ($TiO_2/Ir_{0.7}Ta_{0.3}O_2$/Ti), and a reference electrode (Ag/AgCl) was employed in a single compartment cell with a working volume of 25 mL. The background electrolyte was a 60 mM aqueous solution of Na_2SO_4. The optimum concentration of Na_2SO_4 was found to be 60 mM in terms of electrochemical efficiency (Fig. S1). As a consequence, the electrochemical reactions were primarily run in the 60 mM Na_2SO_4 electrolyte solution. The distance between the anode and cathode was 13 mm. During testing for the simultaneous electrochemical production of H_2O_2 and the concomitant degradation of organic substrates, a constant cathodic potential was applied to the electrodes using a computer-controlled potentiostat (SP-50, BioLogic). An aliquot of a substrate stock solutions (BPA, phenol, and 4-CP) was added to the electrolyte to give an establish a pre-set concentration of the target substrate. The initial pH was adjusted to a set value using either 1.0 M $HClO_4$ or 1.0 NaOH solutions. Oxygen was purged in to the reactor for 30 min before application of a constant potential and then continuously purged during the course of electrolysis. Nitrogen (N_2) gas purging of the aqueous solutions was carried out when low concentrations of dissolved oxygen were required. Aliquots of 1 mL were intermittently withdrawn from the reactor using a 1-mL pipet and were transferred into a glass vial without filtration for the analysis of the concentration of H_2O_2 and organic pollutants. Cyclic voltammetry (CV) data were collected in the Na_2SO_4 solution in the potential range of −0.8 to 0.0 V at a scan rate of 50 mV s^{-1}.

4. Analysis

The concentrations of BPA, phenol, and 4-CP were quantitatively analyzed using a high performance liquid chromatograph (HPLC, Agilent 1100 series) equipped with a Zorbax XDB column. The HPLC measurement was carried out using a binary mobile phase of acetonitrile and phosphoric acid (30%:70% for BPA and 10%:90% for phenol and 4-CP). Chloride produced by 4-CP degradation was monitored using an ion chromatograph (IC, Dionex, USA) with an anion-exchange column (Ionpac AS 19). The total organic carbon (TOC) was analyzed using a TOC analyzer (Aurora TOC). The production of ·OH was

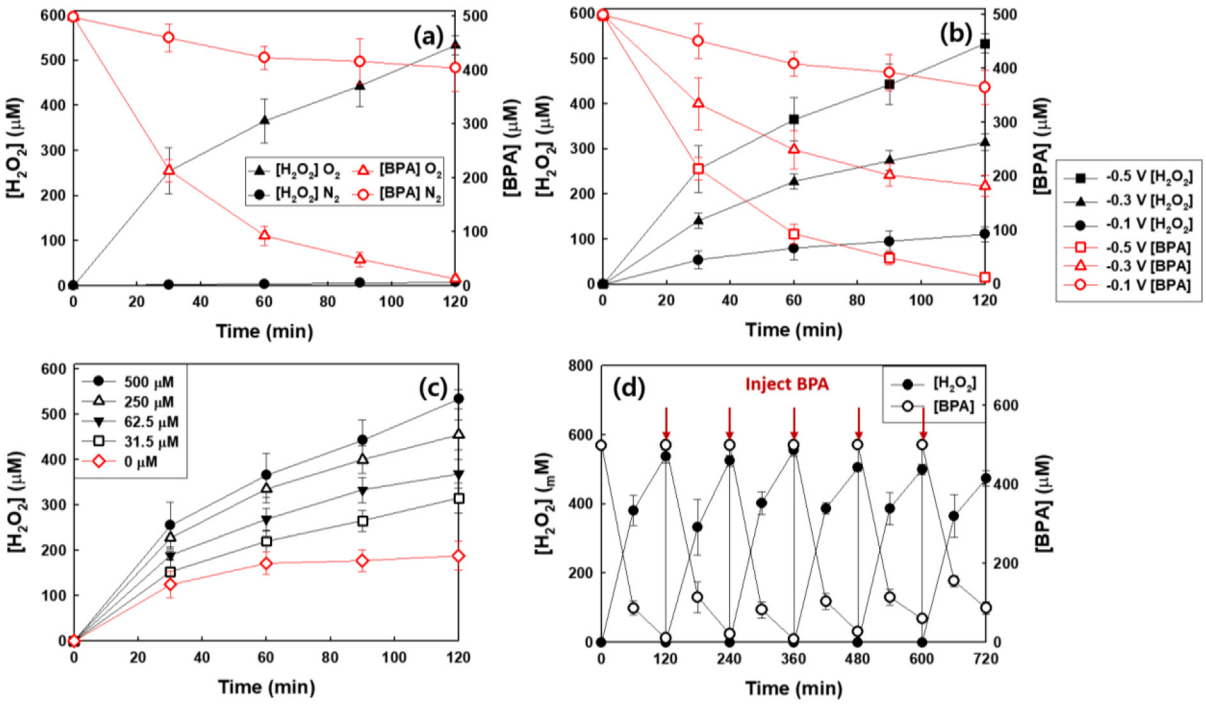

Fig. 1. Time profiles of simultaneous H_2O_2 production and BPA degradation (a) under O_2-or N_2-purged condition and (b) under different applied cathodic voltage. (c) Effect of BPA concentration on the production of H_2O_2. (d) Repeated runs for H_2O_2 production and the concurrent BPA degradation. ($[Na_2SO_4]_0$ = 60 mM; $[BPA]_0$ = 500 μM (for a, b, and d); E_{cell} = −0.5 V (for a, c, and d); pH_i = 3.0; continuously O_2^- or N_2-purged (for a)).

monitored using coumarin as a chemical trap of ˙OH. Coumarin is oxidized by hydroxyl radical to form 7-hydroxycoumarin [20]. The hydroxylated product, 7-hydroxycoumarin, was quantified by measuring the fluorescence emission intensity at λ_{em} = 456 nm after excitation at λ_{ex} = 332 nm·H_2O_2 was determined spectrophotometrically using potassium titanium (IV) oxalate [21]. The absorbance at 400 nm (ε = 9351 mol^{-1} cm^{-1}) was measured using a UV/Visible spectrophotometer (Nanodrop 2000c).

5. Results and discussion

5.1. Simultaneous H_2O_2 production and BPA degradation

Fig. 1a demonstrates that the production of H_2O_2 proceeds simultaneously with BPA degradation in the Na_2SO_4 electrolyte at a constant potential under O_2-purging. Under N_2 purging the production of H_2O_2 was negligibly low as shown in Fig. 1a. Given this result it is clear that H_2O_2 is primarily produced via O_2 reduction at the cathode (Eq. (1)) [11]. This result was confirmed using cyclic voltammetry (Fig. S2). A reduction peak appeared near −0.4 V vs. Ag/AgCl in the presence of O_2 is attributed to the reduction of O_2 leading to the formation of H_2O_2 [22,23]. The reduction peak at −0.4 V disappeared in the N_2-purged solution as observed previously [11,22]. The degradation of BPA was also reduced in the absence of O_2 (Fig. 1a). Fig. 1b shows the production of H_2O_2 coupled with BPA degradation as a function of the applied potential. The efficiencies for the production of H_2O_2 and degradation of BPA were increased with increasing the applied potential. H_2O_2 was not produced in the absence of an external potential bias, whereas the [BPA] was slightly reduced (Fig. S3). This result is most likely due to the adsorption of BPA on to the surface of anode at pH 3. Fig. 1c compares the production of H_2O_2 as a function of the BPA concentration. The electrochemical generation of H_2O_2 was increased with an increasing concentration of BPA. In particular, H_2O_2 was continuously produced in the presence of BPA, whereas its generation reached an apparent steady-state level in the absence of BPA after 1 h of electrolysis. This steady-state is achieved due to the *in situ* decomposition of the H_2O_2 [23]. During repeated electrolytic cycles, a loss of the activity for BPA degradation and H_2O_2 production was not observed four catalytic cycles. However, cycling for more than four cycles resulted in a small loss of activity (Fig. 1d). This result can be ascribed to active site blocking on the electrode surface due to the adsorption of BPA and its reaction product intermediates generated during BPA degradation.

5.2. Influence of BPA on H_2O_2 decomposition

The effects of BPA on the kinetics of decomposition of H_2O_2 were determined by following the change in concentration of 5 mM of hydrogen peroxide in the electrolyte solution in the presence and absence of BPA (Fig. 2a). The decomposition of H_2O_2 in the absence of BPA was faster than that observed in the presence of BPA. Although the decomposition of H_2O_2 was significantly reduced at E_{app} = 0.0 V compared to E_{app} = −0.5 V, it was also found to be faster in the absence of BPA as shown in Fig. S4. The rate constant for H_2O_2 formation and decomposition were treated in terms of zero-order kinetics for production and first-order kinetics for decay, respectively [17]. The formation rate was increased and the decomposition rate was reduced in the presence of BPA compared to the absence of BPA (Fig. 2b). To further clarify the effect of BPA on the production of H_2O_2, excess BPA (1 mM) was added into the electrolyte during the course of electrolysis (after 1 h). The electrochemical production of H_2O_2 was enhanced by 55% (188 → 418 μM at 2 h) and the cathodic current was slightly increased (Fig. 2c) after adding BPA. These results clearly show that the presence of BPA as an anodic electrode donor offsets the *in situ* decomposition of H_2O_2 due to a net higher electrochemical rate of H_2O_2 formation via O_2 reduction in the presence of BPA.

The electrochemically generated H_2O_2 could be decomposed on the surface of either the cathode or the anode (Scheme 1a). However, the cathodic decomposition of H_2O_2 can be excluded since most carbon-based cathodes including the graphite rod used in this study have been found to have low activities for H_2O_2 decomposition [18]. In the case of H_2O_2 decomposition on the anode, we expect to see the formation of

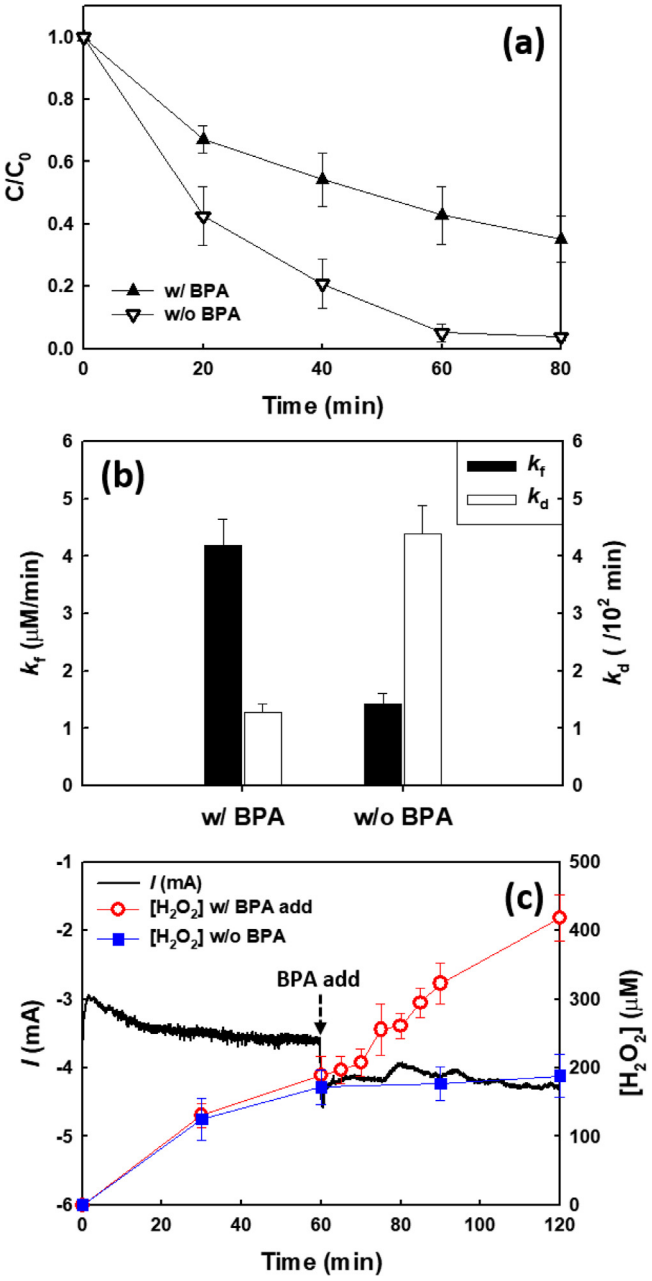

Fig. 2. (a) Decomposition of H_2O_2 and (b) formation rate constant (k_f) and decomposition rate constant (k_d) for H_2O_2 in the presence and absence of BPA. (c) Effect of BPA on H_2O_2 production and cell current. BPA (1 mM) was added to the electrolyte (as indicated by arrows) in the course of electrolysis. ($[Na_2SO_4]_0$ = 60 mM; $[BPA]_0$ = 500 μM (for a and b); $[H_2O_2]_0$ = 5 mM (for a and b); E_{cell} = −0.5 V; pH_i = 3.0; continuously O_2-purged).

hydroperoxo species (≡Ti-OOH) through the adsorption on the protective overlayer of TiO_2 of the anode (reaction (2) in Scheme 1a) [17,25]. We were able to confirm this possibility as shown in Fig. S4. However, we did not observe any noticeable difference and characteristic peaks related with hydroperoxo species in either the Raman or the XPS spectra of the anode before and after electrochemical reactions (*data not shown*). This may be due to the fact that surface-bound hydroperoxyl species are rapidly converted into $HO_2^{\cdot}$ and O_2 (Eqs. (5) and (6) and reaction (3) in Scheme 1a) [24,26]. Furthermore, H_2O_2 is decomposed by $^{\cdot}OH$ generated on the surface of the anode (Eq. (7) and reaction (4) in Scheme 1a) [27]. On the other hand, the anodic decomposition of H_2O_2 appears to be significantly inhibited in the presence of BPA (Scheme 1b). The formation of hydroperoxo species is most likely prevented due to the sorption of BPA is instead of H_2O_2 on the outer surface of the anode (reaction (1) in Scheme 1b and Fig. S3). In addition, BPA acts as a scavenger of $^{\cdot}OH$ (reaction (2) in Scheme 1b) given the second-order rate constant for $^{\cdot}OH + BPA \longrightarrow k = 6.9 \times 10^9$ M^{-1} s^{-1}. In comparison, the corresponding rate constant for $^{\cdot}OH + H_2O_2 \longrightarrow k = 3.2 \times 10^7$ M^{-1} s^{-1} [28]. The competition between the two decomposition pathways in the presence of BPA at the anode surface has net effect of allowing for the solution phase concentration of H_2O_2 to increase with time until reaching a steady-state condition.

5.3. Effect of pH and electrolytes

The rates of H_2O_2 production and BPA degradation as a function of the initial pH of the electrolyte solution are shown in Fig. 3a. From this data, it is clear that the rate of H_2O_2 production decreased with increasing pH. These results may be due to the role of proton coupled electron transfer (PCET) to O_2 (Eq. (1)) [29] leading on the electrochemical formation of H_2O_2 via O_2 reduction at the cathode. The decrease in the rate of BPA degradation was minimal over the pH range of 3–7. However, the degradation rate decreased between pH 9 and 11. The increased in reaction rate with pH can be directly correlated with pK_a of BPA and the corresponding surface charge distribution of the TiO_2 layer of the anode. The deprotonation of BPA (pK_{a1} = 9.6 and pK_{a2} = 10.2 yields the conjugate bases ($HBPA^-$) and (BPA^{2-})) [30] results in an electrostatic repulsion of the anionic BPA species from the negatively charged TiO_2 surface (pH_{pzc} (point of zero charge) ≈ 6.0 [31]) at higher pH. The electrostatic repulsion thus inhibits the adsorption of BPA on the anode surface at higher pH and thus the increased decomposition of H_2O_2. On the other hand, the adsorption of BPA on the anode surface facilitates the degradation of BPA under acidic and circum-neutral pH compared to alkaline pH. Furthermore, competitive adsorption of BPA on the anode surface inhibits the adsorption of H_2O_2 on the anode at lower pH resulting in the reduced anodic decomposition of H_2O_2 (*see* Fig. 2b). The pH-dependent results indicate that low pH conditions are more favorable for the proton-assisted electrochemical production of H_2O_2 coupled with the degradation of BPA.

The impact of the background electrolyte on the rates of H_2O_2 production and BPA degradation was examined as shown in Fig. 3b. The rates of H_2O_2 production and BPA degradation were slightly decreased in the $NaClO_4$ electrolyte solution compared to our reference electrolyte Na_2SO_4. In contrast, the degradation of BPA was enhanced in the NaCl electrolyte solution compared to Na_2SO_4 [32]. The enhanced BPA degradation in a NaCl electrolyte is due to the anodic production of reactive chlorine species (RCS) (*e.g.*, chlorine radical ($Cl^{\cdot}$), dichloride radical anion ($Cl_2^{\cdot -}$), hypochlorous acid (HOCl), and hypochlorite (OCl^-)) oxidatively generated on the surface of anode in the presence of NaCl (Eqs. (8)–(12)) [33,34].

$$> Ti\text{-}OH + h^+ \rightarrow > Ti\text{-}{}^{\cdot}OH + e^- \quad (8)$$

$$> Ti\text{-}{}^{\cdot}OH + Cl^- \rightarrow > Ti\text{-}OH + Cl^{\cdot} \quad (9)$$

$$Cl^{\cdot} + Cl^- \rightarrow Cl_2^{\cdot -} \quad (10)$$

$$> Ti\text{-}{}^{\cdot}OH + Cl^- + H_2O \rightarrow > Ti\text{-}OH + HOCl + H^+ + e^- \quad (11)$$

$$HOCl \rightleftharpoons OCl^- + H^+ \quad (12)$$

Given a sufficient applied potential, electron-hole pairs are formed and migration of a hole (h^+) to a surface titanol group (> TiOH) leads to the formation of surface bound hydroxyl radical. However, the production of RCS has a negative effect on the electrochemical production of H_2O_2. The reactive chlorine species contribute collectively to the decomposition of H_2O_2 (Eqs. (13)–(16)) [27]. In experiments described herein, the decomposition of H_2O_2 was accelerated at a high pH compared to low pH (Fig. S5). It is clear that H_2O_2 reacts faster with

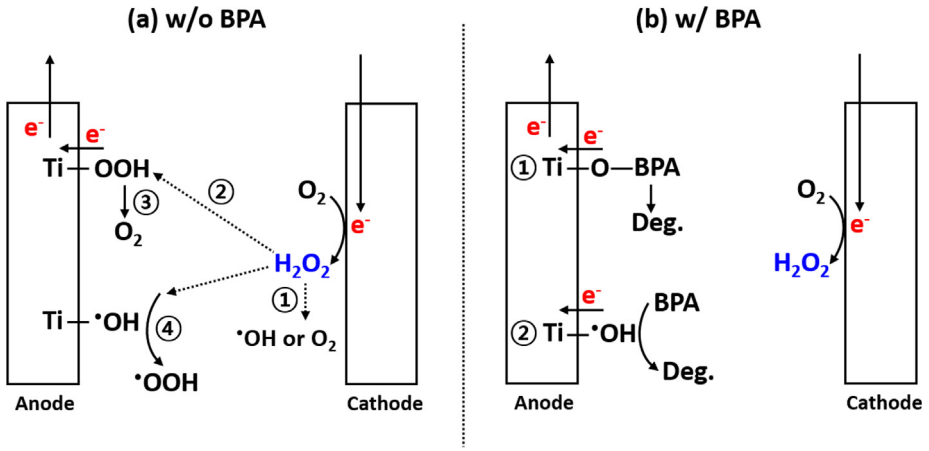

Scheme 1. Schematic illustration of (a) anodic decomposition of *in situ* formed H_2O_2 in the absence of BPA and (b) production of H_2O_2 in the presence of BPA.

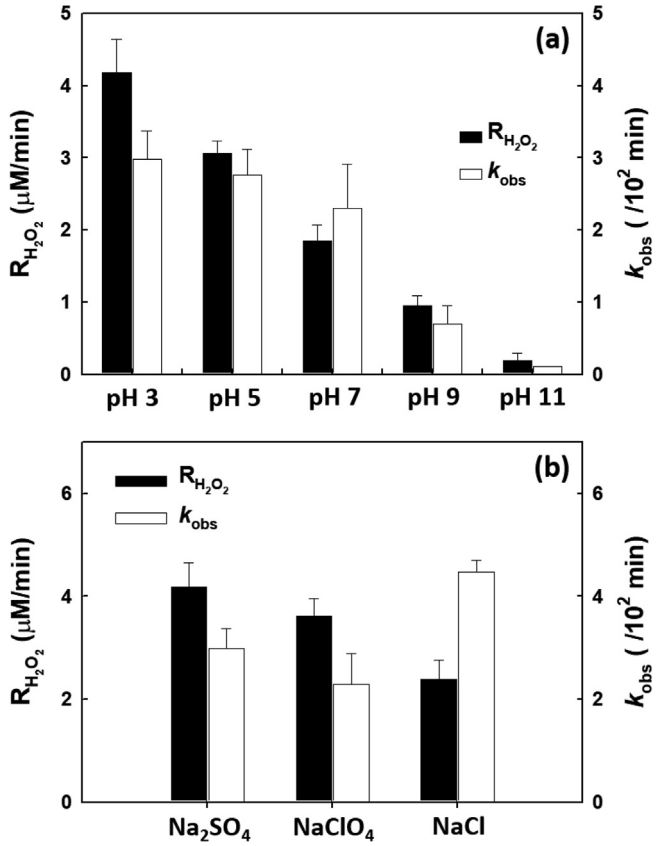

Fig. 3. Effect of (a) initial pH and (b) electrolytes on the kinetic rate of simultaneous H_2O_2 production and BPA degradation. ([electrolyte]$_0$ = 60 mM; [BPA]$_0$ = 500 μM; E_{cell} = −0.5 V; continuously O_2-purged).

RCS (*e.g.*, $^{-}$OCl) under alkaline conditions compared to those at lower pH. For example, the bimolecular rate constant for reaction of H_2O_2 with hypochlorite (HOCl; pK_a = 7.6) (Eq. (12)) is substantially higher at high pH (7.5×10^3 M^{-1} s^{-1}) compared to circum-neutral pH (196 M^{-1} s^{-1}) [35]. Furthermore, the RCS generated on the anode surface are reduced back to chloride on the cathode surface (Eqs. (17)–(20)) [33]. Cathodic chloride reduction is competitive with the reduction of O_2 leading to H_2O_2 production. Therefore, the rate of H_2O_2 production is significantly reduced in the presence of NaCl compared to Na_2SO_4 (Fig. 3b) consistent with the following set of reactions.

$$H_2O_2 + Cl^{\cdot} \rightarrow HOO^{\cdot} + H^+ + Cl^- \quad (13)$$

$$H_2O_2 + Cl_2^{\cdot -} \rightarrow HOO^{\cdot} + H^+ + 2Cl^- \quad (14)$$

$$H_2O_2 + HClO \rightarrow H_2O + O_2 + H^+ + Cl^- \quad (15)$$

$$H_2O_2 + OCl^- \rightarrow Cl^- + O_2 + H_2O \quad (16)$$

$$Cl^{\cdot} + e^- \rightarrow Cl^- \quad (17)$$

$$Cl_2^{\cdot -} + e^- \rightarrow 2Cl^- \quad (18)$$

$$HClO + H^+ + 2e^- \rightarrow Cl^- + H_2O \quad (19)$$

$$OCl^- + H_2O + 2e^- \rightarrow Cl^- + 2OH^- \quad (20)$$

5.4. Mechanism of BPA degradation

Direct electron transfer to a surface-trapped hole may contribute to BPA degradation. In order to confirm this possibility, the cathodic current was measured in the presence and absence of BPA under oxic O_2 and then under anoxic N_2 conditions (Fig. S6). Under these conditions, the cathodic current was slightly increased in the presence of BPA compared to the absence of BPA under both O_2 and N_2. These results imply that direct electron transfer to a surface-trapped hole provides a minor pathway for BPA degradation. The rate of BPA degradation in an $NaClO_4$ electrolyte solution was found to be slightly reduced compared to the same reaction conditions in the Na_2SO_4 electrolyte (*see* Fig. 3b). This result suggests that $SO_4^{\cdot -}$ may have been produced via anodic sulfate oxidation. Another possible oxidant in the system is the surface-bound hydroxyl radical ($^{\cdot}$OH) that is generated via surface titanol group oxidation (*i.e.*, > Ti-OH + h^+) on the hydrated TiO_2 surfaces of anode (Eq. (8)) [27]. To confirm the role of $^{\cdot}$OH, BPA degradation was tested in the presence of *tert*-butanol (t-BuOH) and methanol (MeOH) as preferential radical scavengers of $^{\cdot}$OH and $SO_4^{\cdot -}$, respectively (Fig. 4a). t-BuOH and MeOH have similar bimolecular rate constants for reactions with $^{\cdot}$OH (*e.g.*, 6.0×10^8 M^{-1} s^{-1} and 9.7×10^8 M^{-1} s^{-1}, respectively); however, the rate constant for MeOH + $SO_4^{\cdot -}$ $\longrightarrow$ 3.2×10^6 M^{-1} s^{-1} is higher than that for t-BuOH + $SO_4^{\cdot -}$ $\longrightarrow$ 4.0×10^5 M^{-1} s^{-1} for the reaction with $SO_4^{\cdot -}$ [36,37]. t-BuOH and MeOH react with $^{\cdot}$OH at similar rates, whereas MeOH reacts almost an order of magnitude faster with $SO_4^{\cdot -}$ compared to t-BuOH. The quenching effects of t-BuOH (0.34×10^{-2} min^{-1}) and MeOH (0.25×10^{-2} min^{-1}) for BPA degradation are similar (Fig. 4a). This result demonstrates that BPA is mainly degraded by $^{\cdot}$OH or surface-bound hydroxy radical, > TiOH$^{\cdot}$, which is consistent with the finding that BPA degradation in a Na_2SO_4 solution was similar to that in a $NaClO_4$ solution (*see* Fig. 3b). If BPA is degraded by $SO_4^{\cdot -}$, the quenching effect with MeOH should be greater than that with t-BuOH. However, the BPA degradation kinetics were not completely quenched. This result can be attributed to direct electron transfer to a

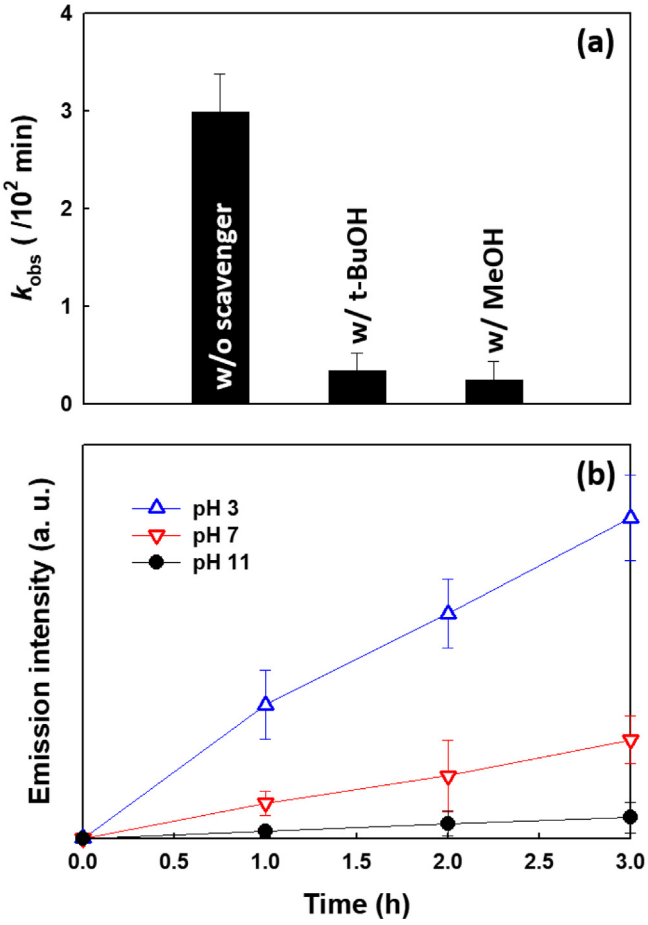

Fig. 4. (a) Effect of t-BuOH and MeOH on BPA degradation. (b) Electrochemical production of coumarin-OH adduct (7-hydroxycoumarin). ($[Na_2SO_4]_0$ = 60 mM; $[BPA]_0$ = 500 μM (for a); $[MeOH]_0$ = [t-BuOH]$_0$ = 100 mM (for a); $[coumarin]_0$ = 1 mM (for b); E_{cell} = −0.5 V; pH_i = 3.0 (for a); continuously O_2-purged).

surface-trapped hole by BPA leading to its degradation. The hypothesis is consistent with results showing a slight increase in the cathodic current in the presence of BPA compared to the absence of BPA under both O_2 and N_2 (*see* Fig. S6).

The generation of ˙OH was further confirmed by using coumarin as a selective probe reagent for ˙OH trapping. The hydroxylated products (7-hydroxycoumarin) generated by the reaction of coumarin with ˙OH (˙OH + coumarin → 7-hydroxycoumarin) was quantified by monitoring the fluorescence emission [38]. Fig. 4b shows the pH-dependent electrochemical production of 7-hydroxycoumarin. The electrochemical production of 7-hydroxycoumarin was increased with decreasing pH, which demonstrates that the electrolytic degradation of BPA can be mainly ascribed to the facile production of ˙OH as a primary oxidant produced on the surface of the anode at lower pH. This observation agrees with the data presented in Fig. 3a, which shows higher electrochemical activities for H_2O_2 production and BPA degradation under acidic and neutral pH compared to alkaline pH conditions. Even though a graphite rod normally has a low activity for catalyzing the decomposition of H_2O_2, the decomposition of H_2O_2 via this pathway (*see* Eq. (3)) cannot be ruled out. To test this possibility, the carbon cathode was replaced by a stainless steel cathode that has a lower activity for the electrochemical production of H_2O_2 than a graphite rod [39]. However, in spite of a significant reduction in the rate of H_2O_2 formation on the stainless steel cathode, the concomitant degradation of BPA was only slightly reduced compared to case of graphite rod cathode (Fig. S7). This result suggests that BPA degradation is initiated by surface-bound > TiOH˙ radicals produced at the anode surface not by free ˙OH radicals produced via H_2O_2 reduction at the cathode.

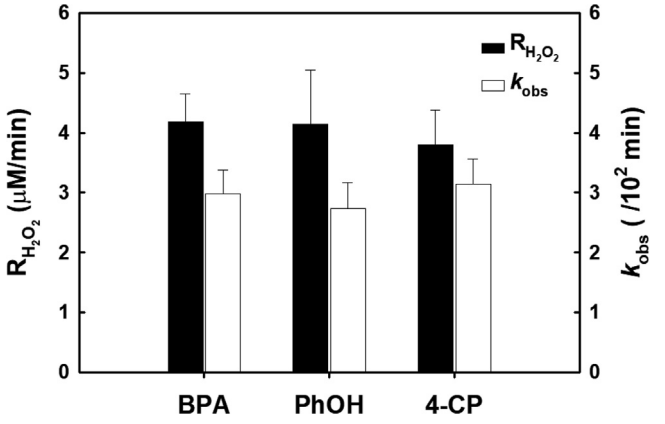

Fig. 5. Simultaneous H_2O_2 production coupled with various phenolic organic pollutants degradation. ($[Na_2SO_4]_0$ = 60 mM; [organic pollutants]$_0$ = 500 μM; E_{cell} = −0.5 V; pH_i = 3.0; continuously O_2-purged).

The pH change observed during electrolysis in the presence of BPA was completely different from that observed in the absence of BPA (Fig. S8). After applying an external bias potential (−0.5 V), the pH immediately increased from 5.8 to 7.5 in the absence of BPA due to the consumption of protons required for H_2O_2 production and then very slightly decreased. On the other hand, the pH was continuously reduced during the oxidation of BPA. This result is due to the formation of organic acids such as lactic, oxalic, fumaric, and glutaric acid [40]. Quinones and catechol were formed as reaction intermediates (Fig. S9a), which were, in turn, oxidized into organic acids. Despite the almost complete removal of BPA in 2 h, the TOC removal was only 66% after 4 h, although complete mineralized was achieve in 6 h (Fig. S9b).

Phenol (PhOH) and 4-chlorophenol (4-CP) were electrolytically oxidized under identical conditions (Fig. 5) and were found to have similar rates degradation and H_2O_2 production compared to BPA. Even though reactive chlorine species were produced in the oxidation of 4-CP (Fig. S10), their effects on H_2O_2 production was minor compared to electrolysis in the NaCl electrolyte (*see* Fig. S5). Thus, we conclude that the RCS concentration produced during the electrolysis of 4-CP was low (< 1 mM) [35].

6. Conclusions

Herein, we clearly demonstrate that positive effect of organic electron donors on the electrochemical production of H_2O_2. The organic substrates are preferentially adsorbed on the anode surface preventing the anodic oxidation of H_2O_2 formed on the cathode. Furthermore, the organic electron donors actively scavenge surface-bound hydroxyl radical (˙OH), which also reacts competitively with H_2O_2. As a result, the oxidative decomposition of H_2O_2 is reduced resulting in the net accumulation of H_2O_2 during the electrolysis of organic pollutants.

Acknowledgement

This research was supported by the Bill and Melinda Gates Foundation (OPP1149755).

Appendix A. Supplementary data

Supplementary data to this article can be found online at https://doi.org/10.1016/j.cej.2019.05.165.

References

[1] J.M. Campos-Martin, G. Blanco-Brieva, J.L.G. Fierro, Hydrogen peroxide synthesis: an outlook beyond the anthraquinone process, Angew. Chem. Int. Ed. 45 (2006) 6962–6984.

[2] H. Kim, Y. Choi, S. Hu, W. Choi, J.H. Kim, Photocatalytic hydrogen peroxide production by anthraquinone-augmented polymeric carbon nitride, Appl. Catal., B 229 (2018) 121–129.

[3] S. Yuan, Y. Fan, Y. Zhang, M. Tong, P. Liao, Pd-catalytic in situ generation of H_2O_2 from H_2 and O_2 produced by water electrolysis for the efficient electro-fenton degradation of rhodamine B, Envion. Sci. Technol. 45 (2011) 8514–8520.

[4] A. El-Ghenymy, J.A. Garrido, F. Centellas, C. Arias, P.L. Cabot, R.M. Rodriguez, E. Brillas, Electro-fenton and photoelectro-fenton degradation of sulfanilic acid using a boron-doped diamond anode and an air diffusion cathode, J. Phys. Chem. A 116 (2012) 3404–3412.

[5] S. Malato, J. Caceres, Degradation of imidacloprid in water by photo-fenton and TiO_2 photocatalysis at a solar pilot plant: a comparative study, Environ. Sci. Technol. 35 (2001) 4359–4366.

[6] Y. Shiraishi, S. Kanazawa, D. Tsukamoto, A. Shiro, Y. Sugano, T. Hirai, Selective hydrogen peroxide formation by titanium dioxide photocatalysis with benzylic alcohols and molecular oxygen in water, ACS Catal. 3 (2013) 2222–2227.

[7] P. Landon, P.J. Collier, A.J. Papworth, C.J. Kiely, G.J. Hutchings, Direct formation of hydrogen peroxide from H_2/O_2 using a gold catalyst, Chem. Commun. 2058–2059 (2002).

[8] J.K. Edwards, G.J. Hutchings, Palladium and gold-palladium catalysts for the direct synthesis of hydrogen peroxide, Angew. Chem. Int. Ed. 47 (2008) 9192–9198.

[9] G. Centi, S. Perathoner, S. Abate, Direct synthesis of hydrogen peroxide: recent advances, in: N. Mizuno (Ed.), Direct Synthesis of Hydrogen Peroxide: Recent Advances, Wiley-VCH, Weinheim, 2009.

[10] N.M. Wilson, D.W. Flaherty, Mechanism for the direct synthesis of H_2O_2 on Pd clusters: heterolytic reaction pathways at the liquid-solid interface, J. Am. Chem. Soc. 138 (2016) 574–586.

[11] Y. Liu, X. Quan, X. Fan, H. Wang, S. Chen, High-yield electrosynthesis of hydrogen peroxide from oxygen reduction by hierarchically porous carbon, Angew. Chem. Int. Ed. 54 (2015) 6837–6841.

[12] X. Shi, S. Siahrostami, G.-L. Li, Y. Zhang, P. Chakthranont, F. Studt, T.F. Jaramillo, X. Zheng, J.K. Nørskove, Understanding activity trends in electrochemical water oxidation to form hydrogen peroxide, Nat. Commun. 8 (2017) 701–706.

[13] T.P. Fellinger, F. Hasché, P. Strasser, M. Antionietti, Mesoporous nitrogen-doped carbon for the electrocatalytic synthesis of hydrogen peroxide, J. Am. Chem. Soc. 134 (2012) 40724075.

[14] I. Yamanaka, T. Murayama, Neutral H_2O_2 synthesis by electrolysis of water and O_2, Angew. Chem. Int. Ed. 47 (2008) 1900–1902.

[15] Y. Sun, I. Sinev, W. Ju, A. Bergmann, S. Dresp, S. Kühl, C. Spöri, H. Schmies, H. Wang, D. Bernsmeier, B. Paul, R. Schmack, R. Kraehnert, B.R. Cuenya, P. Strasser, Efficient electrochemical hydrogen peroxide production from molecular oxygen on nitrogen-doped mesoporous carbon catalysts, ACS Catal. 8 (2018) 2844–2856.

[16] V. Viswanathan, H.A. Hansen, J.K. Nørskov, Selective Electrochemical generation of hydrogen peroxide from water oxidation, J. Phys. Chem. Lett. 6 (2015) 4224–4228.

[17] G.H. Moon, W. Kim, A.D. Bokare, N.-E. Sung, W. Choi, Solar production of H_2O_2 on reduced graphene oxide-TiO_2 hybrid photocatalysts consisting of earth-abundant elements only, Energy Environ. Sci. 7 (2014) 4023–4028.

[18] E. Brillas, I. Sirés, M.A. Oturan, Electro-Fenton process and related electrochemical technologies based on Fenton's reaction chemistry, Chem. Rev. 109 (2009) 6570–6631.

[19] Y. Yang, J. Shin, J.T. Jasper, M.R. Hoffmann, Multilayer heterojunction anodes for saline wastewater treatment: design strategies and reactive species generation mechanisms, Environ. Sci. Technol. 50 (2016) 8780–8787.

[20] M.S. Koo, K. Cho, J. Yoon, W. Choi, Photoelectrochemical degradation of organic compounds coupled with molecular hydrogen generation using electrochromic TiO_2 nanotube arrays, Environ. Sci. Technol. 51 (2017) 6590.

[21] R.M. Sellers, Spectrophotometric determination of hydrogen peroxide using potassium titanium(IV) oxalate, Analyst 105 (1980) 950–954.

[22] C. Walter, K. Kummer, D. Vyalikh, V. Brüser, A. Quade, K.-D. Weltmann, Using a dual plasma process to produce cobalt-polypyrrole catalysts for the oxygen reduction reaction in fuel cells I. Characterization of the catalytic activity and surface structure, J. Electrochem. Soc. 159 (2012) F494–F500.

[23] E. Farjami, M.A. Rottmayer, J.J. Deiner, Evidence for oxygen reduction reaction activity of a $Ni(OH)_2$/graphene oxide catalyst, J. Mater. Chem. A 1 (2013) 15501–15508.

[24] E. Peralta, R. Natividad, G. Roa, R. Martin, R. Romero, T. Pavon, A comparative study on the electrochemical production of H_2O_2 between BDD and graphite cathodes, Sustain. Environ. Res. 23 (2013) 259–266.

[25] V. Maurino, C. Minero, G. Mariella, E. Pelizzetti, Sustained production of H_2O_2 on irradiated TiO_2-fluoride systems, Chem. Commun. 2627–2629 (2005).

[26] E. Brillas, C.A. Martínez-Huitle, Decontamination of wastewaters containing synthetic organic dyes by electrochemical methods. An updated review, Appl. Catal., B 166–167 (2015) 603–643.

[27] H. Park, C.D. Vecitis, M.R. Hoffmann, Electrochemical water splitting coupled with organic compound oxidation: the role of active chlorine species, J. Phys. Chem. C 113 (2009) 7935–7945.

[28] J.R. Peller, S.P. Mezyk, W.J. Cooper, Bisphenol A reactions with hydroxyl radicals: diverse pathways determined between deionized water and tertiary treated wastewater solutions, Res. Chem. Intermed. 35 (2009) 21–34.

[29] Z. Qiang, J.-H. Chang, C.-P. Huang, Electrochemical generation of hydrogen peroxide from dissolved oxygen in acidic solutions, Water Res. 36 (2002) 85–94.

[30] P.S. Yap, T.-T. Lim, M. Lim, M. Srinivasan, Synthesis and characterization of nitrogen-doped TiO_2/AC composite for the adsorption–photocatalytic degradation of aqueous bisphenol-A using solar light, Catal. Today 151 (2010) 8–13.

[31] J. Ryu, W. Choi, Substrate-specific photocatalytic activities of TiO_2 and multiactivity test for water treatment application, Environ. Sci. Technol. 42 (2008) 294–300.

[32] S. Kim, S.K. Choi, B.Y. Yoon, S.K. Lim, H. Park, Effects of electrolyte on the electrocatalytic activities of RuO_2/Ti and Sb–SnO_2/Ti anodes for water treatment, Appl. Catal., B 97 (2010) 135–141.

[33] J. Kim, D. Kwon, K. Kim, M.R. Hoffmann, Electrochemical production of hydrogen coupled with the oxidation of arsenite, Environ. Sci. Technol. 48 (2014) 2059–2066.

[34] X.Y. Yu, Critical evaluation of rate constants and equilibrium constants of hydrogen peroxide photolysis in acidic aqueous solutions containing chloride ions, J. Phys. Chem. Ref. Data 33 (2004) 747–763.

[35] J.M. Barazesh, T. Hennebel, J.T. Jasper, D.L. Sedlak, Modular advanced oxidation process enabled by cathodic hydrogen peroxide production, Environ. Sci. Technol. 49 (2015) 7391–7399.

[36] Y.H. Guan, J. Ma, X.-C. Li, J.-Y. Fang, L.-W. Chen, Influence of pH on the formation of sulfate and hydroxyl radicals in the UV/peroxymonosulfate system, Environ. Sci. Technol. 45 (2011) 9308–9314.

[37] J. Lim, D.-Y. Kwak, F. Sieland, C. Kim, D.W. Bahnemann, W. Choi, Visible light-induced catalytic activation of peroxymonosulfate using heterogeneous surface complexes of amino acids on TiO_2, Appl. Catal., B 225 (2018) 406–414.

[38] K. Ishibashi, A. Fujishima, T. Watanabe, K. Hashimoto, Detection of active oxidative species in TiO_2 photocatalysis using the fluorescence technique, Electrochem. Commun. 2 (2000) 207–210.

[39] E. Vyhnánková, Z. Kozáková, F. Krčma, A. Hrdlička, Influence of electrode material on hydrogen peroxide generation by DC pinhole discharge, Open Chem. 13 (2015) 218–223.

[40] Y.H. Cui, X.-Y. Li, G. Chen, Electrochemical degradation of bisphenol A on different anodes, Water Res. 43 (2009) 1968–1976.